View metadata, citation and similar papers at core.ac.uk
brought to you by CORE
provided by NASA Technical Reports Server

N92-22524

TURBOMACHINERY

Robert J. Simoneau, Anthony J. Strazisar,
Peter M. Sockol, Lonnie Reid,
and John J. Adamczyk

SUMMARY

The discipline research in turbomachinery, which is directed toward building the tools needed to understand such a complex flow phenomenon, is based on the fact that flow in turbomachinery is fundamentally unsteady or time dependent. Success in building a reliable inventory of analytic and experimental tools will depend on how we treat time and time-averages, as well as how we treat space and space-averages. The challenge is to develop a set of computational and experimental tools which genuinely increase our understanding of the fluid flow and heat transfer in a turbomachine. Examples of the types of computational and experimental tools under current development, with progress to date, are examined. The examples include work in both the time-resolved and time-averaged domains.

INTRODUCTION

Because flow in turbomachinery is fundamentally unsteady or time dependent, the discipline research in turbomachinery is directed toward building the tools needed to understand such a complex flow phenomenon. Success in building a reliable inventory of analytic and experimental tools will depend on how we treat time and time-averages, as well as how we treat space and space-averages. The raw tools at our disposal - both experimental and computational - are truly powerful, and their numbers are growing at a staggering pace. As a result of this power, a case can be made that we are currently in a situation where information is outstripping understanding. The challenge is to develop a set of computational and experimental tools which genuinely increase our understanding of the fluid flow and heat transfer in a turbomachine. References 1 to 7 provide some background on the state of the art in developing these tools.

This paper outlines a philosophy based on working on a stairstep hierarchy of mathematical and experimental complexity to build a system of tools that will enable one to aggressively design the turbomachinery of the next century. Examples of the types of computational and experimental tools under current development at Lewis, with progress to date, are examined. The examples include work in both the time-resolved and time-averaged domains.

A CENTRAL THEME OF THE TURBOMACHINERY RESEARCH PROGRAM

The long-range goal of the turbomachinery research program at NASA Lewis is to establish a validated three-dimensional viscous analysis capability for

multistage turbomachinery, including unsteady effects and surface heat transfer. A full range of experimental and computational tools are being brought to bear on this problem in order to genuinely increase our understanding of the fluid flow and heat transfer in a turbomachine. The key to this understanding is the selection and successful application of the right tools for the right job.

A central theme of the turbomachinery research program, illustrated in figure 1, is that everything in a turbomachine is fundamentally unsteady (i.e., time dependent). This time dependency is further complicated by strong random disturbances. We have a choice. We can work in the time domain, which is expensive and time consuming; or we can work in the time-averaged domain, which is cheaper but yields less information. Furthermore, it is not simply an on/off, unsteady/steady situation. The averaging is by steps. Some of the time dependent nature can be averaged out, while some can remain. It is a matter of the time scale (or for that matter the length scale) over which the averaging is performed. Time average does not necessarily mean time independent or "steady". Thus, the question becomes both when and when not to average, and also how to average. A proper balance is required. Ultimately the engineer/designer is most interested in average information, but to get there one must properly handle time.

The levels of complexity associated with the handling are illustrated in figures 2 and 3. The time-accurate, unsteady Navier-Stokes and energy equations, which are capable of resolving all relevant time scales, describe the flow in a turbomachine. These are at the top of the stairs in figure 2. They are the easiest set to formulate, but the most difficult set to solve because they require enormous computer power for the simplest cases. To ease the solution a variety of averages are taken. The critical step is to average properly by using the proper time and length scales. Each averaging step results in a loss of information or resolution in the equations, introduces more unknowns, and requires external input (obtained by experiment and by solving the exact equations for simpler cases). One can use engineering judgement to determine how much information is needed to complete the mathematical description of the particular problem at hand. The averaged equations allow this introduction of engineering judgement. The pure unaveraged Navier-Stokes equations must be solved in their entirety.

Similarly in the experimental arena, as illustrated in figure 3, both time-resolved and time-averaged measurements are essential to a full understanding of turbomachinery flow and heat-transfer characteristics. As with analysis, the problem is in determining which technique to apply and when to apply it. Frequently, an average result offers more insight than time-accurate detail. A qualitative visual observation may be crucial to understanding the essential physics. At other times, such a measurement may bury the essential physics. Traditionally, dynamic measurements have provided less accurate absolute measurements than average measurements. Recent improvements suggest that averaging time-resolved measurements may be more accurate than making average measurements, especially in heat transfer. Laser anemometry, in addition to offering the well-known nonintrusive advantage, has an especially nice feature of providing ensemble averages of the random statistics while retaining and identifying the deterministic time dependency. Ultimately, all levels are needed to do the job. The challenge is to choose the right tool for the right job.

The average passage equation system, developed by Adamczyk and coworkers (refs. 8 to 10), is an example of averaging the Navier-Stokes equations. The three momentum equations and the energy equation are subjected to three averaging steps: one to remove random unsteadiness, a second to remove unsteadiness associated with blade-passing frequency and, finally, one to account for the uneven airfoil count from row to row. At its most fundamental level the averaging process introduces 11 unknowns in the axial momentum equation alone, as shown below. The advantage is that the resulting equation set is much easier to solve mathematically. It will be necessary to conduct physical and/or numerical experiments to provide the correlations which bring closure to these equations. The properly averaged equations provide the framework for a large research effort into understanding the physics of fluid flow and heat transfer in turbomachines.

AXIAL MOMENTUM EQUATION:

$$\frac{\partial}{\partial t_1}\lambda_1\bar{\bar{\rho}}\,\tilde{\tilde{r}}\tilde{\tilde{V}}_z + \frac{\partial}{\partial r}\lambda_1 r\bar{\bar{\rho}}\tilde{\tilde{V}}_r\tilde{\tilde{V}}_z + \frac{\partial}{\partial \theta}\lambda_1\bar{\bar{\rho}}\tilde{\tilde{V}}_\theta\tilde{\tilde{V}}_z + \frac{\partial}{\partial z}\lambda_1\left(\bar{\bar{\rho}}\tilde{\tilde{V}}_z\tilde{\tilde{V}}_z + \bar{\bar{P}}\right)$$

CONVECTIVE TERMS

TRANSIENT TERM

$$= \frac{\partial}{\partial r}\lambda_1\left(r\bar{\bar{\tau}}_{rr} - r\,\overline{\hat{\rho}\hat{V}_r\hat{V}_z} - r\,\overline{\bar{\rho}}\,\overline{V_r''V_z''} - r\rho\overline{V_r'V_z'}\right)$$

$$+ \frac{\partial}{\partial \theta}\lambda_1\left(\bar{\bar{\tau}}_{\theta z} - \overline{\hat{\rho}\hat{V}_\theta\hat{V}_z} - \overline{\bar{\rho}}\,\overline{V_\theta''V_z''} - \rho\overline{V_\theta'V_z'}\right)$$

DIFFUSIVE TERMS

$$+ \frac{\partial}{\partial z}\lambda_1\left(\bar{\bar{\tau}}_{zz} - r\,\overline{\hat{\rho}\hat{V}_z\hat{V}_z} - r\,\overline{\bar{\rho}}\,\overline{V_z''V_z''} - r\rho\overline{V_z'V_z'}\right)$$

BODY FORCE TERMS

$$+ F_{IN}^{(ZR)} + F_V^{(ZR)} + F_{IN}^{(ZS)} + F_V^{(ZS)}$$

THE SUCCESSIVE OVERBARS REPRESENT AVERAGING OUT:
(1) RANDOM UNSTEADINESS
(2) PERIODIC UNSTEADINESS
(3) UNEQUAL BLADE COUNT

An example of a calculation using the average passage system of equations (ref. 10) depicts the evolution of a total-temperature distortion through the space shuttle main engine (SSME) fuel pump turbine, as shown in figure 4. The total-temperature profiles are color coded, with red denoting regions of hot gas and blue denoting regions of cold gas. At this stage in the development of the average passage equation system, many of the unknown viscous correlations remain to be determined and are set equal to zero for this calculation. The equations do, however, properly account for the interaction between blade rows. These results show that inviscid mixing as a result of streamwise vorticity generation can produce significant temperature differences between the suction and pressure side of a blade. This difference can lead to local regions of high thermal stress which can cause blade failure. The ability to capture the physics associated with this inviscid mixing process is a key element in increasing the durability of turbine blading.

Similarly the proper experimental tools must be developed and applied. High-speed turbomachinery research facilities are characterized by high-speed rotating machines, small blade-passage heights, three-dimensional flows, transonic velocity levels, high noise and vibration levels, and restricted mechanical access. Because of its high spatial and temporal resolution and nonintrusive nature, laser anemometry has become the measurement method of

choice for obtaining the detailed data required to assess the accuracy and sensitivity of flow analysis codes. In order to overcome the long measurement times required by laser anemometers and to capitalize on the detailed nature of the data which they generate, computer control of data acquisition and real-time data reduction and display, as illustrated in figure 5, are required. NASA Lewis is recognized as a world leader in the development and application of computer-controlled laser anemometer systems for use in both rotating and nonrotating turbine and compressor research applications. The work is summarized in reference 11.

Karman vortex streets are known to exist in blunt-body wakes over a wide flow regime. However, the existence of vortex streets in transonic fan and compressor-blade wakes was not generally anticipated since these blades have thin trailing edges. Laser anemometer measurements obtained in the wake of a transonic fan blade indicated two distinct states of the flow in the central portion of the blade wake - a high-velocity state and a low-velocity state. This behavior is consistent with that which would be displayed by a Karman vortex street. A simple vortex street model was constructed in an attempt to explain the experimental measurements. The model qualitatively agreed with the bimodal character of the velocity measurements. The model was also used to explain, for the first time, the highly unsteady nature of high-response pressure measurements made in the same wake flowfield. This research, which was a cooperative effort with MIT, typifies the manner in which advanced measurements coupled with simple modeling improve our understanding of complex flow phenomena. This work is summarized in figure 6, with details available in reference 12.

RESEARCH IN THE TIME-RESOLVED DOMAIN

Referring back to figure 1, a few examples of research in the time-resolved domain are presented to illustrate the physics which can be identified with time-resolved measurements and analyses. Measurements of the unsteady flowfield within a compressor stator operating downstream of a transonic fan rotor have been obtained using laser anemometry (refs. 13 to 15). Figure 7 shows a contour plot of the ensemble-averaged unresolved unsteadiness in the stator (which includes unsteadiness due to both turbulence and vortex shedding) for one rotor/stator relative position. Areas of high unresolved unsteadiness contain fluid which is in the rotor-blade wake. As the rotor blades rotate past the stator blades, the rotor wakes are convected through the stator row by the absolute flow velocity and, subsequently, chopped by the stator blades. Data obtained at additional times during the blade-passing cycle have been used to produce a movie sequence which illustrates the ensemble-averaged wake dynamics and its effect on the stator flowfield. We have the tools to measure temporal behavior in generic equivalents of a real machine.

A simulation was performed by Whitfield et al. (ref. 16) of the flow through a supersonic throughflow fan stage. This machine differs from today's machinery in that the axial Mach number is supersonic. For supersonic cruise, it offers an improvement in performance over transonic machinery. The three-dimensional simulation highlighted the rotor-stator interaction which occurs at design operating conditions. One of the interactions under study is the formation of "hot spots" at the leading edge of the stator, shown in figure 8. An animation illustrating the processes has also been made. The "hot spots" are at a temperature which exceeds the instantaneous total temperature

(absolute) of the flow stream exiting the rotor. Their formation is believed to be caused by the motion of the shock wave eminating from the pressure surface of the stator. We have the tools to compute temporal behavior in a real machine.

NASA is also developing rotor/stator interaction viscous flow codes (refs. 17 and 18). A quasi-three-dimensional viscous code used to solve for the flow in an isolated turbomachinery blade row was modified to handle equal pitch stator/rotor interaction computations (ref. 17). The solution procedure has been applied to the first-stage turbine rotor of the space shuttle main engine (SSME) fuel turbopump. For this calculation, shown in figure 9, the upstream stator was scaled so that its pitch matched that of the rotor, and the pitch-to-chord ratio remained unchanged. A converged periodic solution was obtained after the stator had seen 10 passing rotor blades or 10 pitch rotations of the rotor, which takes about 2.5 hr on the Cray. Mach contours are shown in the figure for an equal pitch stator/rotor configuration. The average inlet Mach number to the upstream stator is 0.15. The wake region that develops behind the stator passes through the grid interface and is seen in the rotor computational domain. Currently, the analysis is being applied to multiple passages of a single-stage turbine. The stage airfoil configuration is two upstream stators followed by three rotors. The airfoil geometries are taken from the first stage of the SSME fuel turbopump and are scaled to 2:3 from their actual 41:63 airfoil ratio. The details of such interactions are important to our understanding of turbomachinery flows.

EFFECT OF WAKES ON LAMINAR-TURBULENT TRANSITION IN A TURBINE STAGE

Detailed phase-resolved heat-flux data have been obtained on the blade of a full-stage rotating tubine by Dunn (refs. 19 and 20) for Teledyne Corp. in conjunction with a Vane-Blade Interaction program sponsored by the Air Force. A shock tube is used as a short-duration source of heated air, and platinum thin-film gages are used to obtain the heat-flux measurements. Some thin-film gages can be seen figure 10(a) in a leading-edge insert. Heat-flux results are presented in figure 10(b) for the midspan at several locations along the suction surface from stagnation point to 78-percent wetted distance. Each phase-resolved plot represents the ensemble-average of about four to five vane-wake (or passage) crossings. The rapid decrease in heat flux level from stagnation point to trailing edge is evident, as well as the fluctuating laminar-to-turbulent (and back to laminar) component, as the rotor cuts the stator wakes. This high-frequency oscillation from laminar to turbulent flow has important implications for turbine heat-transfer analysis and can only be identified with sophisticated sensors, electronics, and dynamic signal analysis.

As a result of several recent studies, the nature and significance of wake-related flow unsteadiness in turbomachinery blading and its profound effect on heat transfer are beginning to be recognized. In particular, the enhancement of heat transfer to the stagnation region is of interest because of the critical importance of heat transfer in this region. The effect of free-stream turbulence on time-average stagnation region heat transfer has been well documented. However, very few measurements have been obtained of the time-resolved effects of wake passage on heat transfer and the relationship of these effects to the corresponding velocity fluctuations. Current efforts (refs. 21 and 22 and unpublished work by J.E. O'Brien and S.P. Capp are aimed

at obtaining such measurements and performing statistical analysis to determine correlations between the unsteady velocity and heat-flux records. Figure 11 shows a schematic of the rotor-wake rig and representative fluctuating velocity measurements. In addition, stagnation region unsteady heat-flux records are shown which reveal the high degree of heat-transfer enhancement associated with each wake-passing event.

Since gas-side heat-transfer coefficients can vary by an order of magnitude within the transition region, a detailed understanding of boundary-layer transition is critical to the design of effective turbine-airfoil cooling schemes. This is particularly important when one realizes that such events can occur at blade-passing frequency. The present research (ref. 23) is aimed at understanding the fundamental differences between the "classical" boundary-layer transition process and the "bypass" transition process which occurs when a laminar boundary layer is perturbed by large free-stream disturbances. The time-resolved hot wire velocity measurements obtained at a grid-generated free-stream turbulence level of only 0.7 percent, shown in figure 12, indicate a bypass of small disturbances and the rapid development of a turbulent boundary layer as the flow progresses down the plate.

RESEARCH IN THE TIME-AVERAGED DOMAIN

Again, referring to figure 1, a few examples of research in the time-averaged domain are presented to illustrate the composite results which can be obtained from averaged measurements and analyses. As an example (refs. 24 to 26), a photograph of the experimental color temperature patterns of high-resolution, liquid-crystal thermography (figure 13) shows complex contours of constant temperature obtained from an experimental technique in which a uniformly heated turbine-vane cascade endwall surface is operated in an air flow. The resulting isotherms on the test surface are also lines of constant heat-transfer coefficient. The photographic data are then digitized for computer-based processing and display to show color contours of Stanton Number (nondimensional heat-transfer coefficient). The highest heat transfer rates occur in the vane stagnation region (shown in red). This computer-generated display can be used for direct comparison with code-generated predictions. Complex phenomena such as these require complex analyses - the three-dimensional Navier-Stokes codes.

A three-dimensional Navier-Stokes analysis code (RVC3D) is being developed for turbomachinery blade rows (ref. 27). The Navier-Stokes equations are written in a body-fitted coordinate system rotating about the x-axis. Streamwise viscous terms are neglected by using the thin-layer assumption, and turbulence effects are modeled with the Baldwin-Lomax eddy viscosity. The equations are discretized by using finite differences, and solved by using a multistage Runge-Kutta algorithm with a spatially varying time step and implicit residual smoothing. Calculations have been made of a horseshoe vortex formed at the junction of a turbulent endwall boundary layer and a blunt fin, as shown in figure 14. This geometry is to be tested experimentally later this year in an experiment described in the next paragraph. The calculations were done on 65 by 33 by 25 grid (lower figure) at the nominal tunnel operating conditions (Mach number, 0.6; fin thickness Reynolds number, 260 000; inlet boundary-layer thickness, 1 in.). Total pressure contours, 0.025 in. above the endwall, show the primary vortex core (center figure). Vector plots on the upstream symmetry plane (upper left) and on a downstream cross-channel plane (upper right) show the development of a double vortex system. The calculations

required about 1 million words of storage and 10 min of CPU time on a Cray X-MP.

A new facility for fluid mechanics and heat-transfer research, shown in figure 15, will provide benchmark quality experimental data for internal flow code validation. Focus will be on the three-dimensional interaction of the intersecting model with the surface plate (i.e., the horseshoe vortex). The facility will have the following capabilitities: (1) maximum Mach number of 0.6, (2) no tunnel side-wall boundary layers, (3) controllable boundary layer on top and bottom walls of the tunnel, and (4) low inlet turbulence (less than 0.5 percent). The first phase of the experiment will consist of three parts: (1) fluid mechanics measurements will be taken by using a five-hole probe and hot film shear-stress gauges, (2) various flow visualization techniques will be used to define the flow path at the intersecting surfaces, and (3) heat transfer data will be recorded by the liquid crystal technique. The second phase of the work, to be conducted in about two years, will include full flow-field measurements by laser anemometry. This experiment and the RVC3D code development form a critical partnership to the successful development of a turbomachinery analysis capability.

Another complex geometry, the centrifugal compressors feature large surface area and small exit-passage heights. Viscous flow effects, therefore, have a major impact on the flowfield within centrifugal compressors. The inability to accurately predict and measure these flows contributes in large part to the inherently lower efficiency of centrifugal compressors relative to axial-flow compressors.

The large low-speed centrifugal compressor shown in the background of figure 16 has been designed (ref. 28) specifically to provide flow modeling and viscous code-validation data for centrifugal compressors. The impeller was designed to be aerodynamically similar to high-performance, high-speed centrifugal compressors such as the small 6:1 pressure-ratio impeller shown in the photograph. The low-speed impeller has a tip diameter of 60 in. and a design rotational speed of 1920 rpm. Inlet and exit blade heights are 8.70 and 5.4 in., respectively. The large size and low speed of the new impeller generate viscous flow regions (such as blade and endwall boundary layers) and tip clearance flows which are large enough to measure in detail with laser anemometry.

To analyze such geometries an efficient Navier-Stokes analysis code (RVCQ3D) (ref. 5) has been developed for turbomachinery. The effects of radius change, stream surface thickness, and rotation are included, which allows calculations of centrifual impellers, radial diffusers, and axial machines with contoured endwalls. The unsteady Navier-Stokes equations are solved in finite-difference form by using an explicit Runge-Kutta algorithm with a spatially varying time step and multigrid convergence acceleration. The flow in the 6:1 pressure-ratio centrifugal impeller of figure 16 has been calculated on a 161 by 33 grid. Relative Mach number contours (figure 17(a)) show a supersonic bubble on the leading edge terminated by a shock. Rotational effects make the suction-surface boundary layer thin, the pressure-surface boundary layer thick, and they cause the wake to leave the trailing edge in a spiral. The calculations required about 3 million words of storage and 1.5 min of CPU time on a Cray X-MP. The flow in the new, large low-speed rig has also been calculated and is shown in figure 17(b). The ability to validate this

and other codes in the large low-speed rig will generate confidence in the high-speed calculations where validation is near to impossible.

In order to fully validate the codes, they must be shown capable of capturing real physics in real machines. An example is the shock behavior in a transonic fan. Many axial fan and compressor design systems currently in use do not account for passage shock three-dimensionality. In addition, preliminary blade designs are often performed as two-dimensional calculations on blade-to-blade stream surfaces. An assessment of the shock three-dimensionality in transonic rotors is therefore necessary in order to properly account for three-dimensional effects in the design process. Shock locations determined from laser anemometer measurements (ref. 29) are shown on blade-to-blade surfaces of revolution in the upper half of figure 18. Three different views of the same data, as displayed on a graphics workstation, are shown in the lower half of figure 18. A significant spanwise lean of the shock surface is evident in these three-dimensional views.

Increased emphasis on sustained supersonic cruise or hypersonic cruise has revived interest in the supersonic throughflow fan as a possible component in advanced propulsion systems. Use of a fan that can operate with a supersonic inlet axial Mach number is attracive from the standpoint of reducing the inlet losses incurred in diffusing the flow from a supersonic flight Mach number to a subsonic one at the fan face. The data base for components of this type is practically nonexistent, and design of any experiment to study feasibility of this concept must rely heavily on advanced computational tools to enhance the possibility of success. Computer codes that have been developed for design and analysis of transonic turbomachines were modified to allow calculations of blade rows with supersonic inlet Mach numbers (refs. 30 and 31). An inviscid/viscous code and a parabolized viscous code were used to design and analyze the variable nozzle and variable diffuser necessary for the experiment. Off-design analysis of the various components of the experiment indicated that all components would operate as expected over the flow and speed range of the experiment. Figure 19 shows the results obtained for the inlet variable nozzle which sets up the inlet flowfield, the fan rotor, and the variable diffuser, which decelerates the flow toward the collector inlet. All components were analyzed with two different codes in order to give increased confidence in the computed results. This is the ultimate goal of the turbomachinery program - to develop the tools which allow us to push beyond our experience with confidence.

CONCLUDING REMARKS

A complete and mature program has research at all levels along the computational and experimental paths. In the NASA Lewis turbomachinery program, special emphasis is placed on the analytic range from the ensemble (Reynolds) averaged Navier-Stokes equations to the average passage equations. The experimental emphasis is on high-response time-resolved measurements and on real machinery laser anemometry measurements. It is important to emphasize that the successful application of these tools will require a strong interaction between the computational and experimental paths. This concept for developing the tools we need is illustrated in figure 20.

REFERENCES

1. Simoneau, R.J.: Heat Transfer in Aeropropulsion Systems. Heat Transfer in High Technology and Power Engineering, W.J. Yang and Y. Mori, eds., Hemisphere Publishing Corp., Washington, D.C., 1985, pp. 285-319. (NASA TM-87066.)

2. McNally, W.D.; and Sockol, P.M.: Computational Methods for Internal Flows with Emphasis on Turbomachinery. J. Fluids Eng., vol. 107, no. 1, Mar. 1985, pp. 6-22.

3. Povinelli, L.A.: Assessment of Three-Dimensional Inviscid Codes and Loss Calculations for Turbine Aerodynamic Computations. J. Eng. Gas Turbines Power, vol. 107, no. 2, Apr. 1985. pp. 265-275.

4. Rai, M.M.: Navier-Stokes Simulations of Rotor/Stator Interaction Using Patched and Overlaid Grids. J. Propulsion Power, vol. 3, no. 5, Sept.-Oct. 1987, pp. 387-396.

5. Chima, R.V.: Explicit Multigrid Algorithm for Quasi-Three-Dimensional Viscous Flows in Turbomachinery. J. Propulsion Power, vol. 3, no. 5, Sept.-Oct. 1987, pp. 397-405.

6. Davis, R.L.; Ni, R.H.; and Carter, J.E.: Cascade Viscous Flow Analysis Using the Navier-Stokes Equations. J. Propulsion Power, vol. 3, no. 5, Sept.-Oct. 1987, pp. 406-414.

7. Hah, C.: Calculation of Three-Dimensional Viscous Flows in Turbomachinery with an Implicit Relaxation Method. J. Propulsion Power, vol. 3, no. 5, Sept.-Oct. 1987, pp. 415-422.

8. Adamczyk, J.J.; Mulac, R.A.; and Celestina, M.L.: A Model for Closing the Inviscid Form of the Average-Passage Equation System. J. Turbomachinery, vol. 108, no. 2, Oct. 1986, pp. 180-186.

9. Adamczyk, J.J.: A Model Equation for Simulating Flows in Multistage Turbomachinery. ASME Paper 85-GT-226, Mar. 1985.

10. Mulac, R.A., et al.: The Utilization of Parallel Processing in Solving the Inviscid Form of the Average-Passage Equation System for Multistage Turbomachinery. AIAA Paper 87-1108, June 1987. (NASA TM-89845.)

11. Strazisar, A.J.: Laser Fringe Anemometry for Aero Engine Components. Advanced Instrumentation for Aero Engine Components, AGARD CP-399, AGARD, Neuilly-Sur-Seine, France, 1986, pp. 6-1 to 6-32. (Avail. NTIS, AD-A182954.)

12. Hathaway, M.D., et al.: Rotor Wake Characteristics of a Transonic Axial-Flow Fan. AIAA J., vol 24, no. 11, Nov. 1986, pp. 1802-1810.

13. Hathaway, M.D.: Unsteady Flows in a Single-Stage Transonic Axial-Flow Fan Stator Row. NASA TM-88929, 1986.

14. Suder, K.L., et al.: Measurements of the Unsteady Flow Field Within the Stator Row of a Transonic Axial-Flow Fan. I - Measurement and Analysis Technique. ASME Paper 87-GT-226, May 1987.

15. Hathaway, M.D., et al.: Measurements of the Unsteady Flow Field Within the Stator Row of a Transonic Axial-Flow Fan. II - Results and Discussion," ASME Paper 87-GT-227, May 1987.

16. Whitfield, D.L., et al.: Three-Dimensional Unsteady Euler Solutions for Propfans and Counter-Rotating Propfans in Transonic Flow. AIAA Paper 87-1197, June 1987.

17. Jorgenson, P.C.E.; and Chima, R.V.: An Explicit Runge-Kutta Method for Unsteady Rotor/Stator Interaction. AIAA Paper 88-0049, Jan. 1988. (NASA TM-100787.)

18. Rai, M.M.: Unsteady Three-Dimensional Navier-Stokes Simulations of Turbine Rotor-Stator Interaction. AIAA Paper 87-2058, June 1987.

19. Dunn, M.G.; and Hause, A.: Measurement of Heat Flux and Pressure in a Turbine Stage. J. Eng. Power, vol. 104, no. 1, Jan. 1982, pp. 215-223.

20. Dunn, M.G., et al.: Phase-Resolved Heat-Flux Measurements on the Blade of a Full-Scale Rotating Turbine. ASME Paper 88-GT-173, June 1988.

21. O'Brien, J.E., et al.: Unsteady Heat Transfer and Direct Comparison to Steady-State Measurements in a Rotor-Wake Experiment. Heat Transfer 1986, Vol. 3, C.L. Tien et al., eds., Hemisphere Publishing Corp., Washington, D.C., 1986, pp. 1243-1248.

22. O'Brien, J.E.: Effects of Wake Passing on Stagnation Region Heat Transfer. Heat Transfer in Gas Turbine Engines and Three-Dimensional Flows, E. Elovic, J.E. O'Brien, and D.W. Pepper, eds., ASME, 1988, pp. 17-28.

23. Suder, K.L.; O'Brien, J.E.; and Reshotko, E.: Experimental Study of Bypass Transition in a Boundary Layer. NASA TM-100913, 1988.

24. Hippensteele, S.A.; Russell, L.M.; and Stepka, F.S.: Evaluation of a Method for Heat Transfer Measurements and Thermal Visualization Using a Composite of a Heater Element and Liquid Crystals. J. Heat Trans., vol. 105, no. 1, Feb. 1983, pp. 184-189.

25. Hippensteele, S.A.; and Russell, L.M.: High Resolution Liquid-Crystal Heat-Transfer Measurements on the Endwall of a Turbine Passage with Variations in Reynolds Number. NASA TM-100827, 1988.

26. Boyle, R.J.; and Russell, L.M.: Experimental Determination of Stator Endwall Heat Transfer. ASME Paper 89-GT-219, June 1989, NASA TM-101419.

27. Chima, R.V.; and Yokota, J.W.: Numerical Analysis of Three-Dimensional Viscous Internal Flows. NASA TM 100878, 1988.

28. Wood, J.R.; Adam, P.W.; and Buggele, A.E.: NASA Low-Speed Centrifugal Compressor for Fundamental Research. AIAA Paper 83-1351, June 1983. (NASA TM-83398.)

29. Wood, J.R.; Strazisar, A.J.; and Simonyi, P.S.: Shock Structure Measured in a Transonic Fan Using Laser Anemometry. Transonic and Supersonic Phenomena in Turbomachines, AGARD CP-401, AGARD, Neuilly-Sur-Seine, France, 1987, pp. 2-1 to 2-14. (Avail. NTIS, AD-A182996.)

30. Wood, J.R., et al.: Application of Advanced Computational Codes in the Design of an Experiment for a Supersonic Through-Flow Fan Rotor. ASME Page 87-GT-160, June 1987. (NASA TM-88915.)

31. Schmidt, J.F., et al.: Supersonic Through-Flow Fan Design. AIAA Paper 87-1746, June 1987. (NASA TM-88908.)

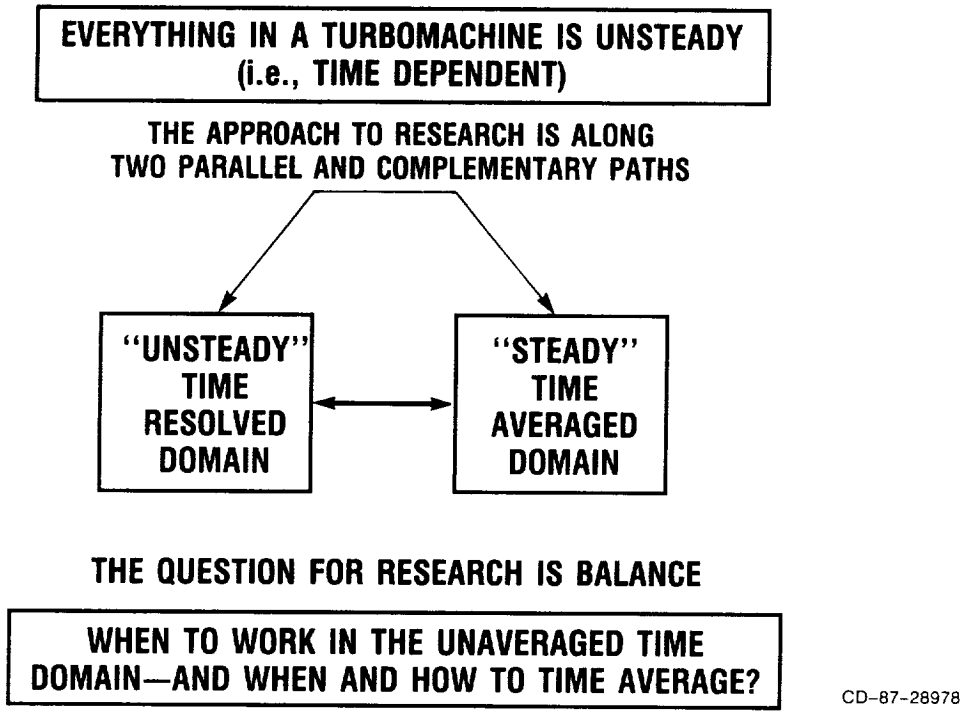

Figure 1. - Central theme for turbomachinery research.

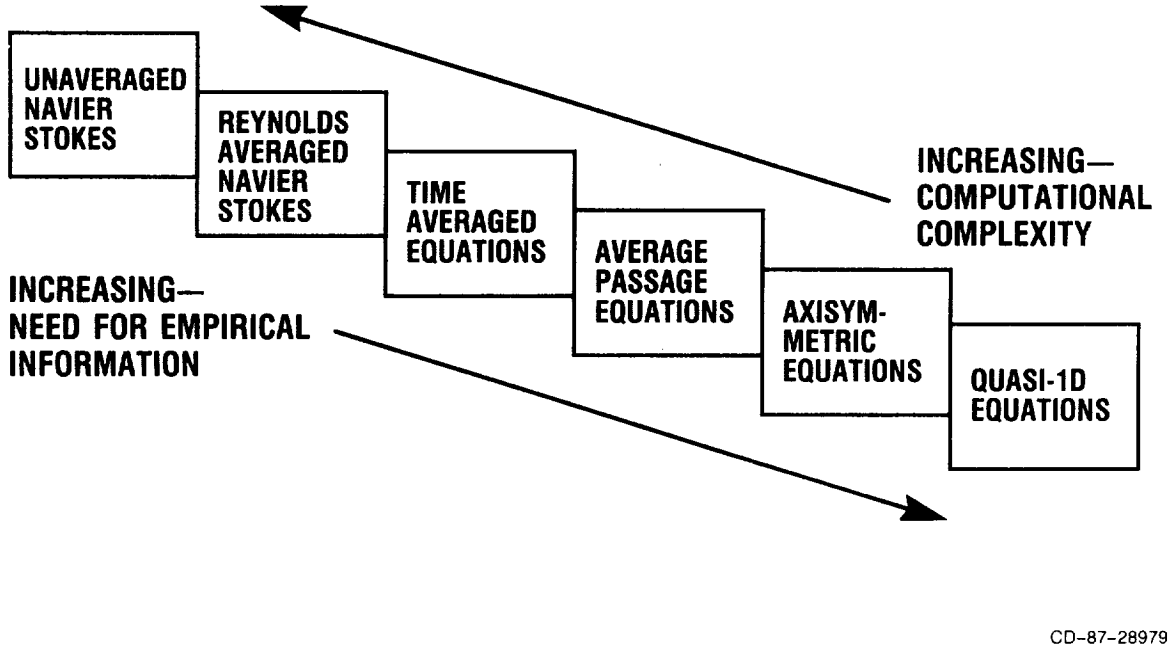

Figure 2. - Levels of complexity along the path of computational analysis.

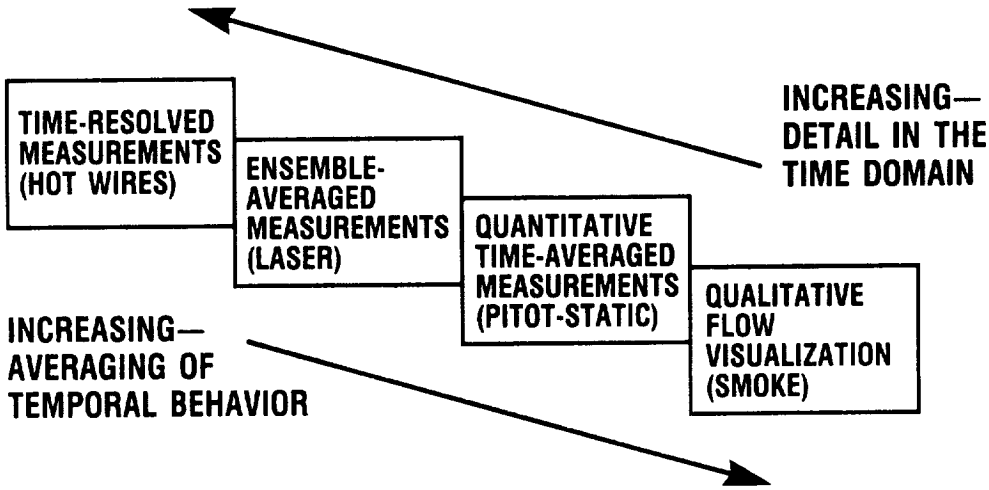

CD-87-28980

Figure 3. - Levels of a complexity along the path of experimental measurements.

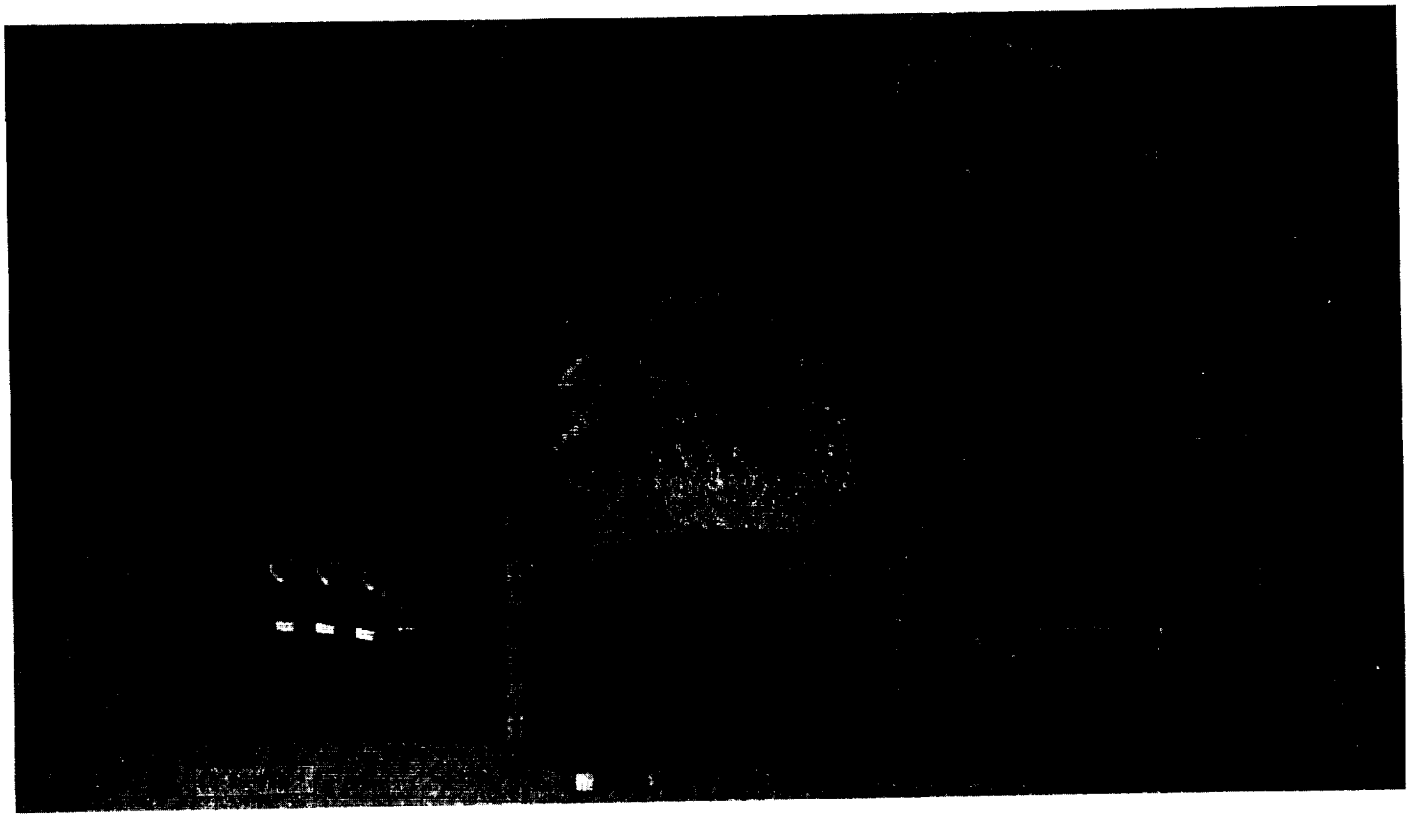

Figure 4. - Evolution of total temperature field within SSME fuel turbine.

ORIGINAL PAGE IS
OF POOR QUALITY

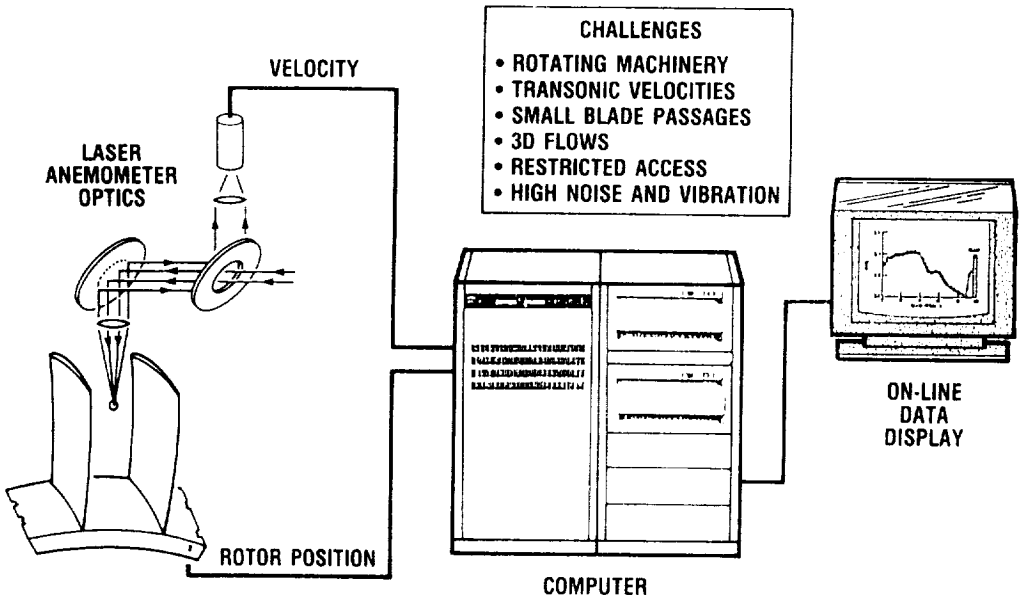

Figure 5. - Turbomachinery laser anemometry systems.

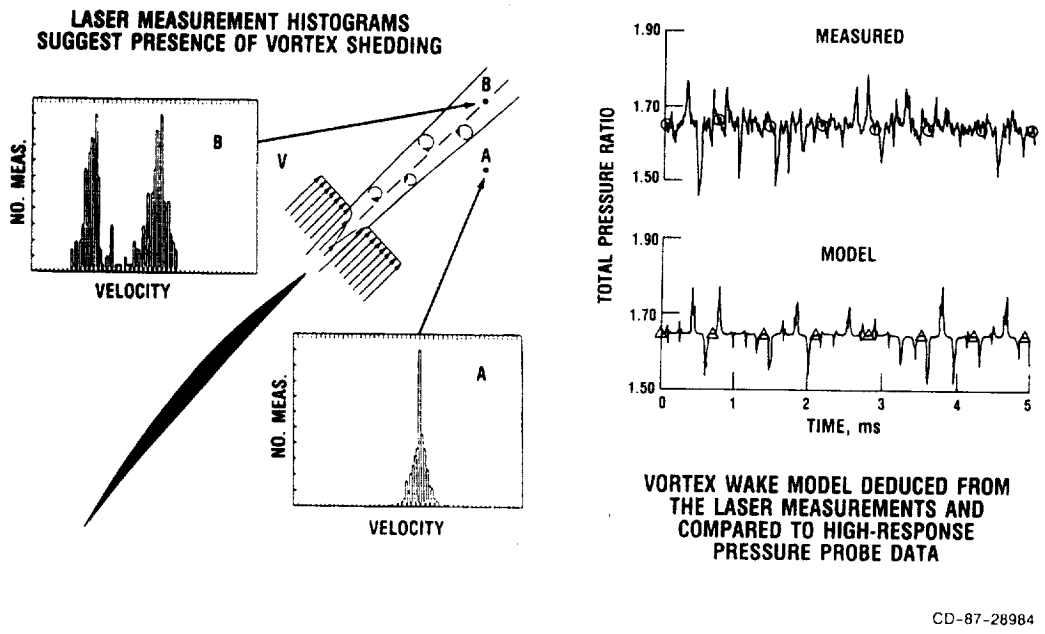

Figure 6. - Developing models to explain flow physics.

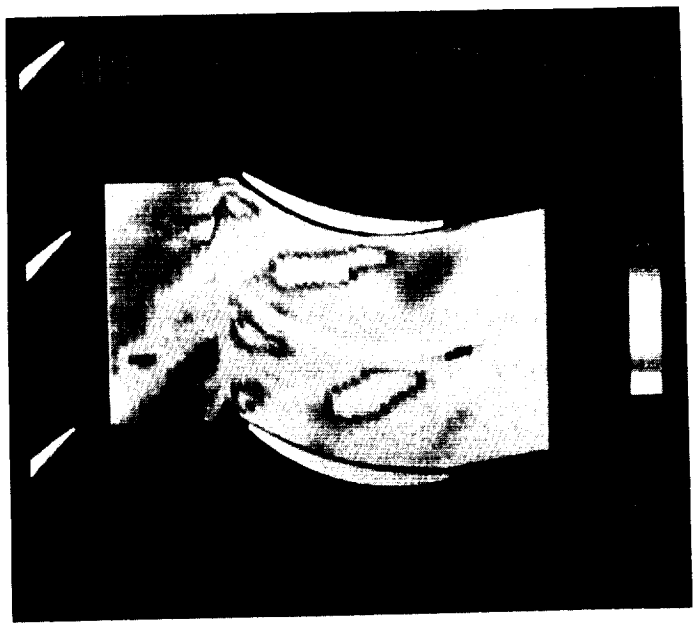

CD-87-28986

Figure 7. - Compressor "turbulent" kinetic energy distribution (one frame from data movie showing progress of wake through stator passage downstream of rotor).

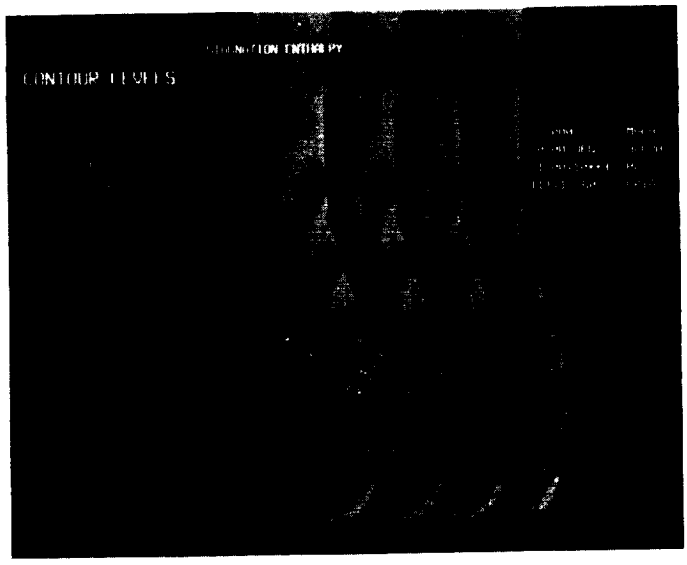

CD-87-28987

Figure 8. - Unsteady Euler calculation for a supersonic throughflow fan (one frame from computational movie showing progress of supersonic rotor exit total temperature through downstream stator).

ORIGINAL PAGE
BLACK AND WHITE PHOTOGRAPH

TIME ACCURATE 2D NAVIER-STOKES CALCULATION, SHOWING THE MACH CONTOUR DISTRIBUTION AT ONE INSTANT OF TIME IN A BLADE-PASSING PERIOD

CD-87-28988

Figure 9. - Rotor/stator interaction calculation - SSME fuel turbine.

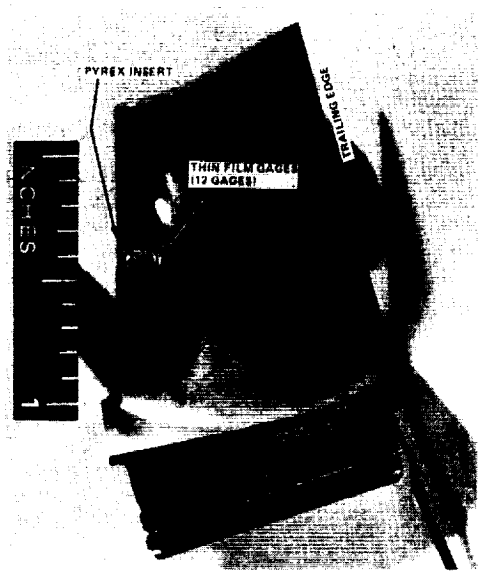

PHOTO OF A ROTOR BLADE INSTRUMENTED WITH THIN-FILM SENSORS

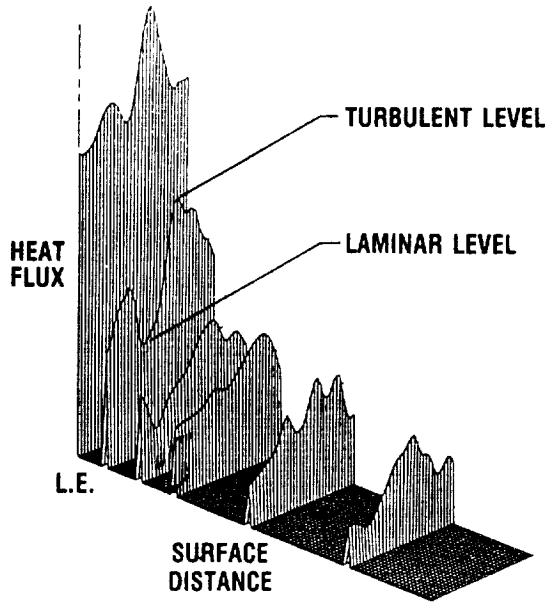

PHASE-RESOLVED CONTOUR PLOT SHOWING THE PROGRESSION OF TRANSITION ALONG THE AIRFOIL

CD-87-28989

Figure 10. - Effect of wakes on laminar-turbulent transition in a turbine stage.

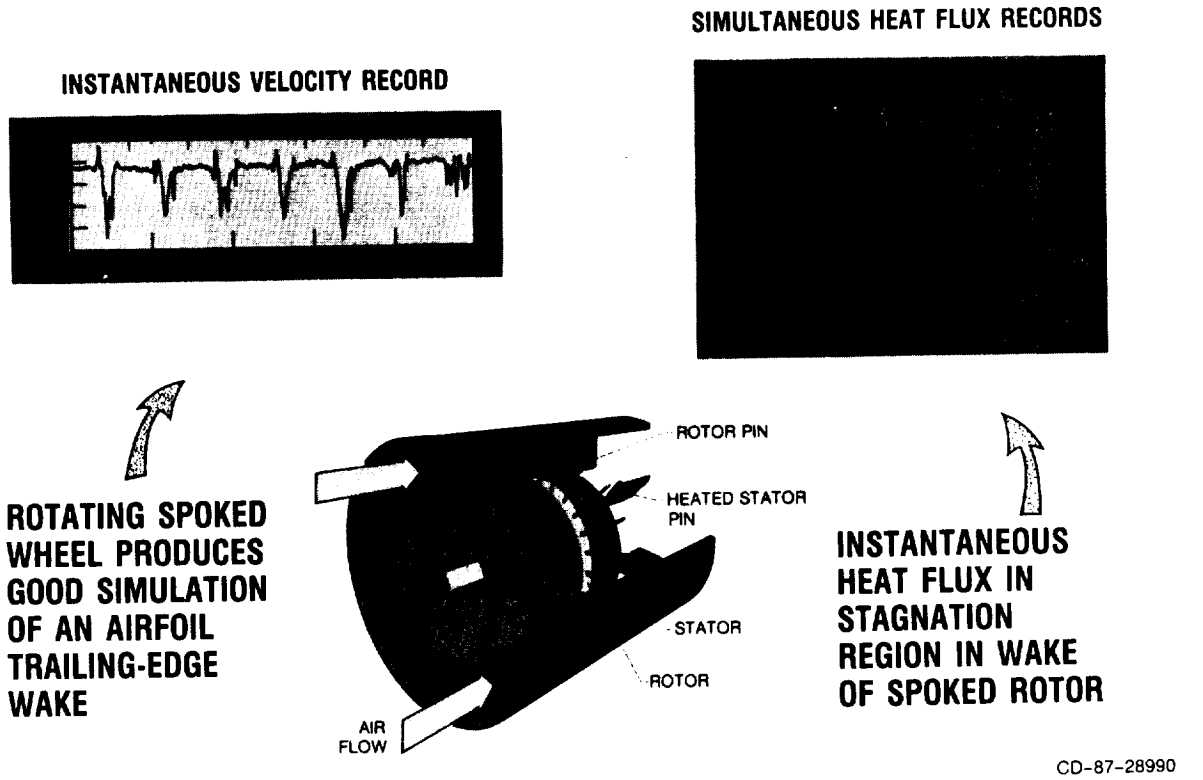

Figure 11. - Unsteady heat transfer in rotor-wake flows.

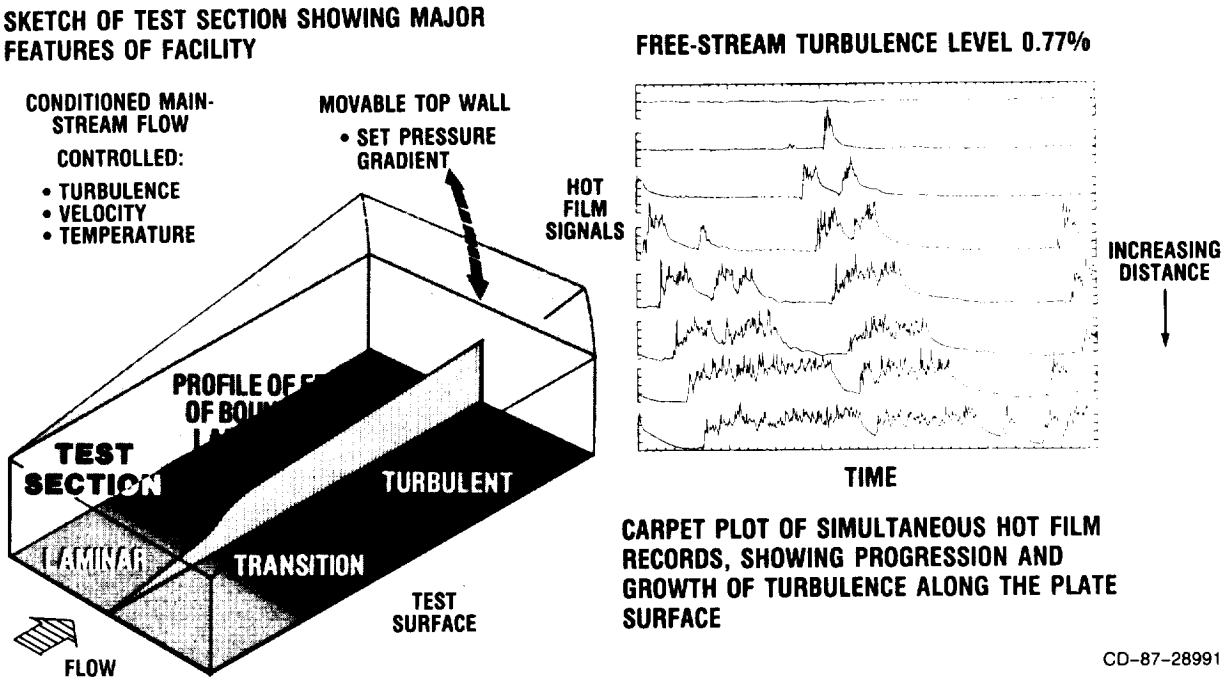

Figure 12. - Boundary-layer transition reserach - a study of intermittent behavior.

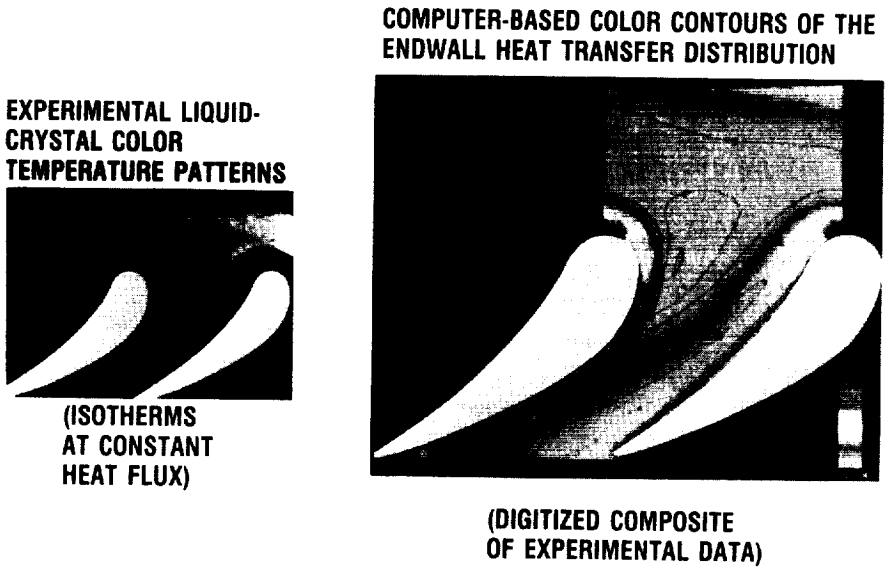

Figure 13. - High-resolution, liquid-crystal turbine endwall heat-transfer data.

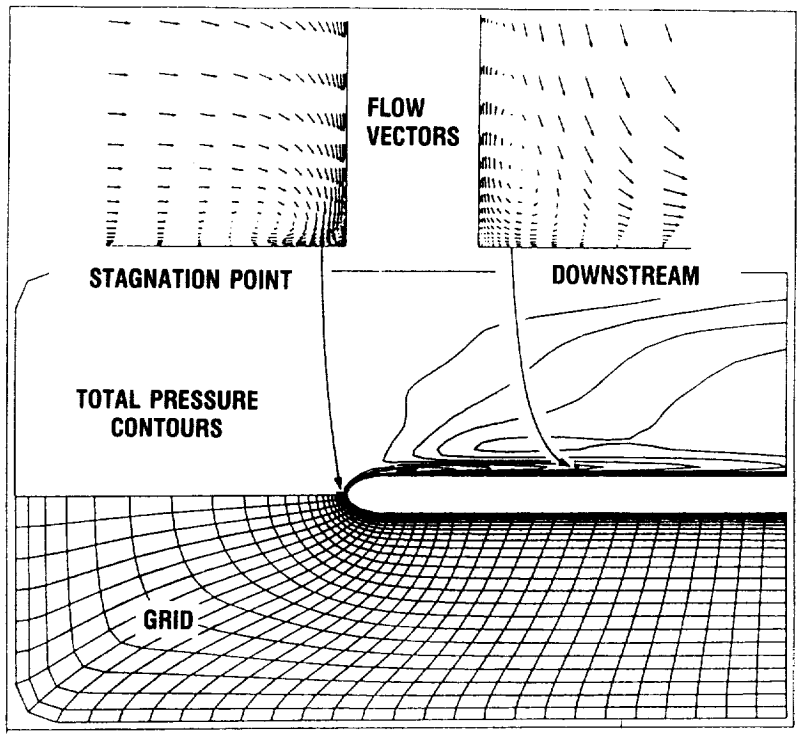

Figure 14. - Three-dimensional Navier-Stokes code analysis of turbulent horseshoe vortex.

ORIGINAL PAGE
BLACK AND WHITE PHOTOGRAPH

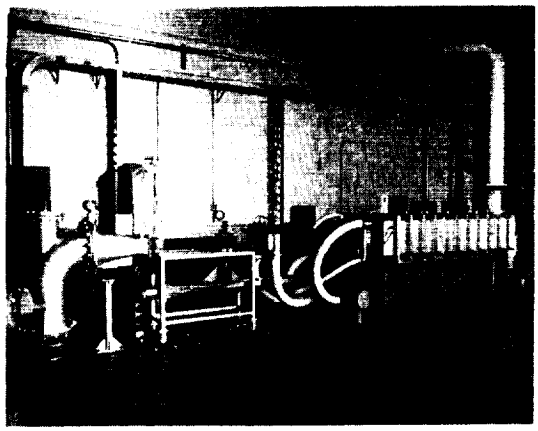

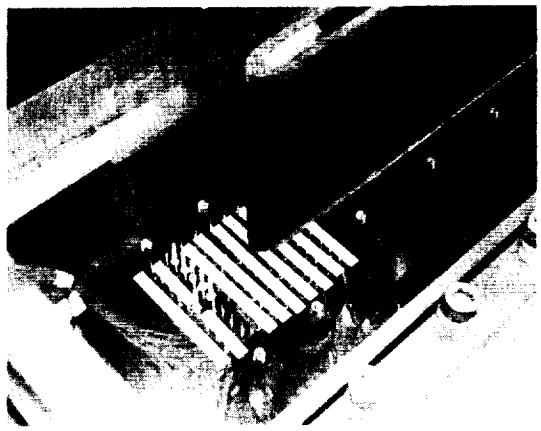

OBJECTIVE

TO OBTAIN DATA TO VERIFY COMPUTATIONAL FLUID MECHANICS COMPUTER CODES THAT ARE CAPABLE OF SOLVING FULLY 3D FLOWS INCLUDING HEAT TRANSFER

CD-87-28995

Figure 15. - Three-dimensional compressible flow tunnel.

UNDERSTANDING THE FLOW PHYSICS AND THE VALIDATION OF COMPLEX TURBOMACHINERY 3D NAVIER-STOKES CODES REQUIRES VERY LARGE ROTATING MACHINERY IN ORDER TO BE ABLE TO EXAMINE THE VISCOUS BOUNDARY LAYERS

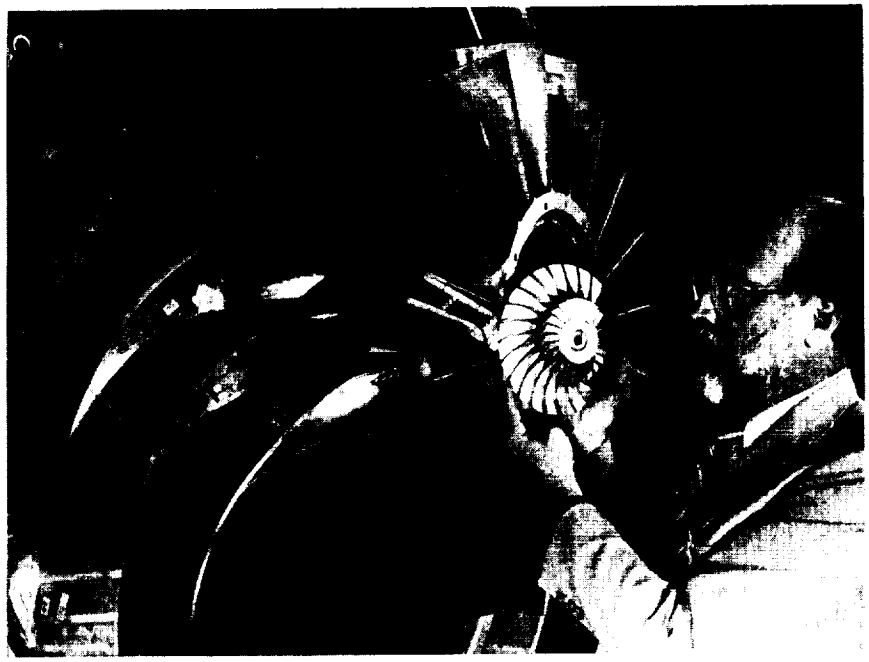

SIZE COMPARISON BETWEEN LOW-SPEED IMPELLER AND 2-LB/S HIGH-SPEED IMPELLER

CD-87-28996

Figure 16. - Large low-speed certrifigal compressor - new flow physics and code validation rig.

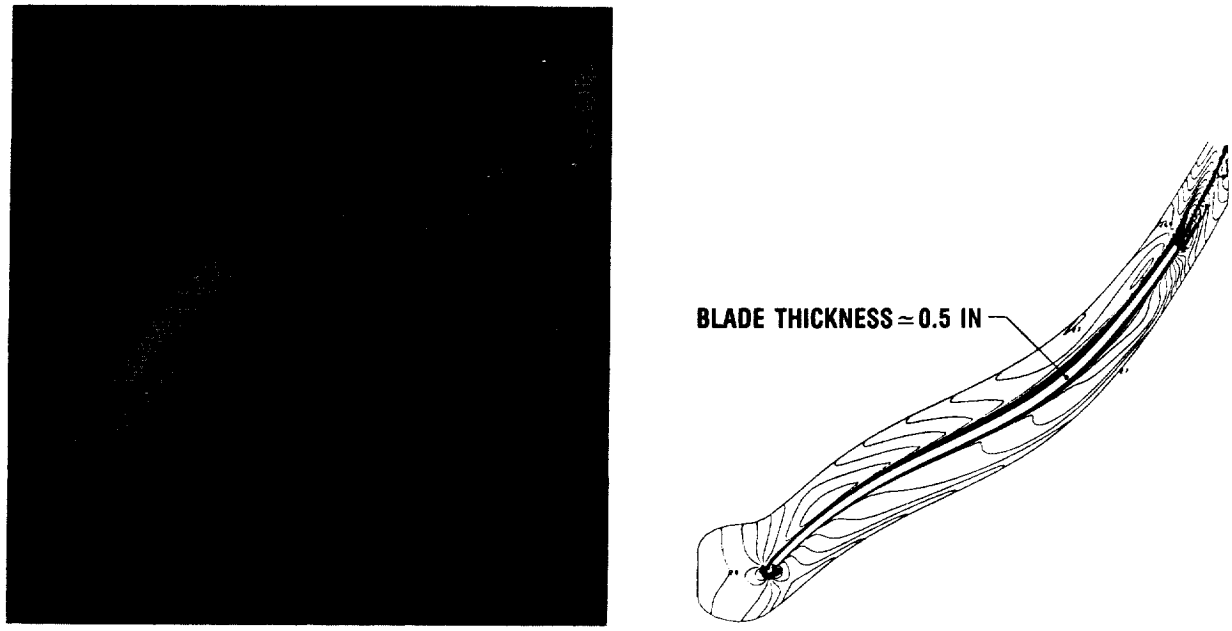

Figure 17. - Quasi-three-dimensional Navier-Stokes code for turbomachinery analysis.

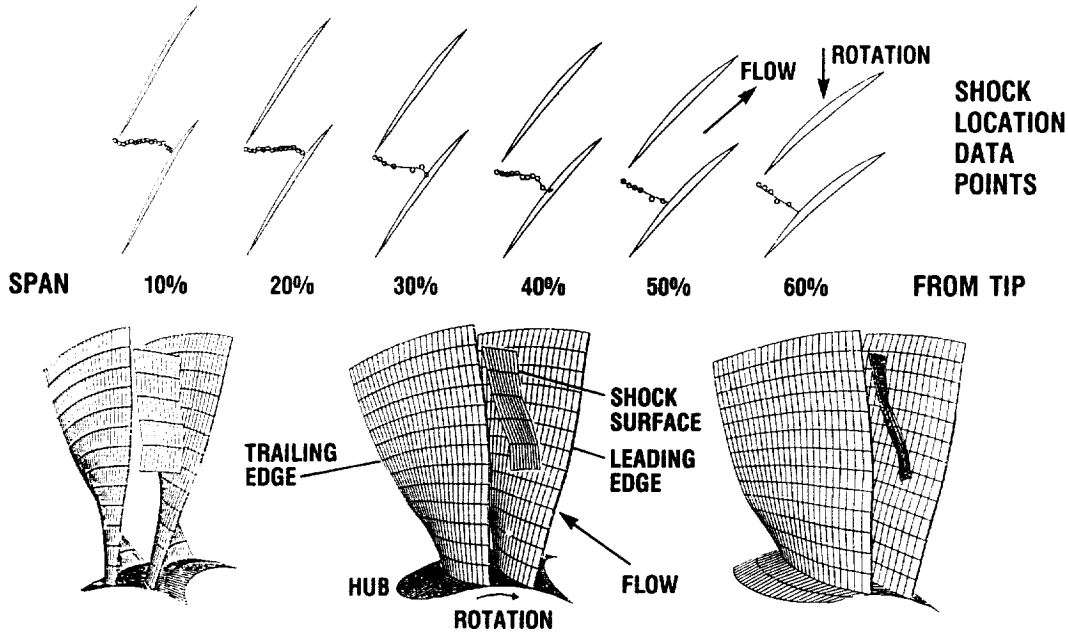

Figure 18. - Measurement of three-dimensional shock structure in transonic axial-flow fan.

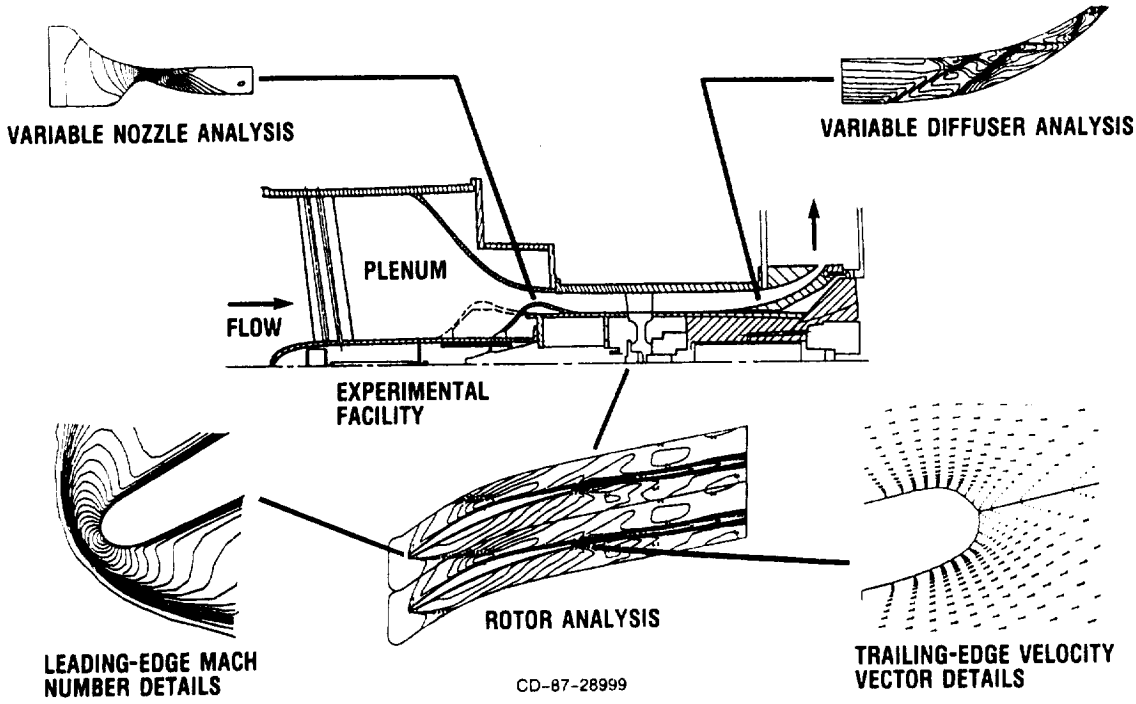

Figure 19. - Application of advanced codes for design of supersonic throughflow fan experiment.

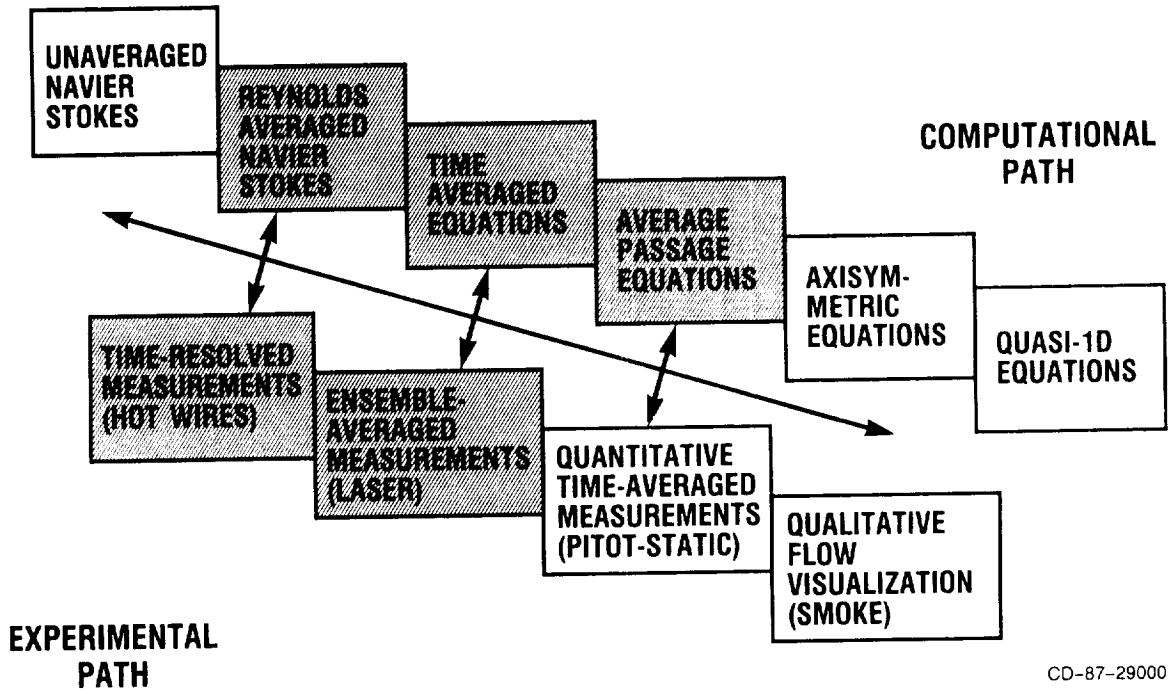

Figure 20. - Position of turbomachinery research program on computational and experimental paths.